Spherical Near-Field Measurements of Satellite Antennas at Extreme Temperatures

A. Giacomini, V. Schirosi, A. Martellosio, L.J Foged
MICROWAVE VISION ITALY
00071 Pomezia (Rome), ITALY
andrea.giacomini@mvg-world.com

M. Moscetti Castellani, D. Cardoni, A. Maraca, F. Rinalducci
ANGELANTONI TEST TECHNOLOGIES
06056 Massa Martana (PG), ITALY
marco.moscetticastellani@angelantoni.it

C. Feat, J. Sinigaglia, S. Leroy, F. Viguier
THALES ALENIA SPACE
31037 Toulouse (FRANCE)
christian.feat@thalesaleniaspace.com

L. Rolo
EUROPEAN SPACE AGENCY, ESTEC,
2200 AG, Noordwijk Zh, THE NETHERLANDS
luis.rolo@esa.int

***Abstract* — Antenna systems commonly used in space applications, are often exposed to extreme environmental conditions and to significant temperature variation. Thermal stress may induce structural deformations of the radiators or affect the RF performance of the active front-ends. These are some of the reasons that pushed the testing technology to characterize the radiating proprieties of Antennas Under Test (AUT) in realistic thermal conditions. Testing facilities available for these purposes are nowadays typically limited in terms of temperature range, measurable radiation pattern and size of the AUT. This paper describes the multi-physics design considerations (i.e. thermal, structural and RF) for the development of a novel facility to evaluate AUT radiation pattern characteristics in thermal conditions, from L to Q band, as an add-on feature to the ESA-ESTEC Hybrid European RF and Antenna Test Zone (HERTZ), located in Noordwijk (The Netherlands). The goal is to extend such a testing to AUTs up to 2.4m diameter in envelope over an extreme temperature range (+/- 120°C), allowing a free movement of the AUT and taking advantage of Spherical Near-Field (SNF) measurement techniques.**

I. INTRODUCTION

Remote sensing systems for Earth observation, antennas for Space Science and novel active antennas for Telecommunications require an accurate characterization of their radiating proprieties before deployment. This typically includes radiation pattern, directivity and gain. For the experimental characterization of such antennas, the Spherical Near-Field (SNF) antenna measurement technique is considered the most accurate way of testing satellite antennas [1]. In its traditional form, the SNF measurement technique is based on acquiring amplitude and phase data points over a spherical surface of constant radius around the Antenna Under Test (AUT). The spacing between these points is dependent on the operating frequency and the radius of the minimum sphere that fully encloses the AUT. There are several ways to implement a motion that allows sampling the field on a spherical surface around the AUT. The most common is to keep the sampling probe stationary and move the AUT in a Roll over Azimuth positioner system (Phi over Theta) [2] [3] [4].

For a large majority of satellite missions, antennas are exposed to significant temperature variations due to sun pointing, sun eclipses and proximity to large albedos. In addition, new technology in active antennas is enabling the use of direct radiating arrays with integrated front-ends and amplification stages that feature complex thermal and structural designs, without affecting their Radio Frequency (RF) performance. These are some of the reasons that pushed testing technology to allow the characterization of the radiating proprieties of antennas under different thermal conditions. These existing systems allow to measure a portion of the radiating characteristics of the antenna but have a common weakness: they do not allow a free movement of the AUT that enables sampling over the full sphere. For this reason, a great interest for antenna measurement in thermal condition arose among the space community in the last years. This interest is focused towards the possibility of adding innovative capabilities on the existing spherical range facilities.

The approach proposed in this paper consists of a RF transparent, thermally insulated dome surrounding the Antenna Under Test (AUT), connected to a thermal unit that allows heating up to +120°C and cooling down to -120°C the AUT. The target operational bandwidth of the facility is 0.4 – 50 GHz. Such a system should allow the free rotation of the Phi and Theta Axis, while cooling or warming the AUT during a SNF acquisition (Figure 1.).

II. SYSTEM DESIGN

Ideally a dome should appear totally transparent to any electromagnetic signal received or transmitted, providing low reflections, low transmission loss and minimum distortion of polarization-dependent antenna patterns. Nevertheless, it must

provide high mechanical robustness with adequate safety margins, acceptable weight and the required thermal insulation.

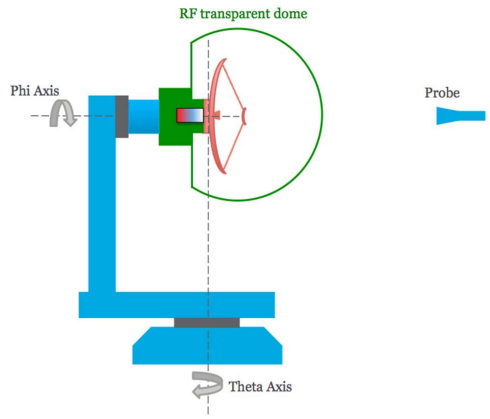

Figure 1. Concept of the antenna testing over temperature stand-alone system

Unfortunately, electrical and mechanical performance are often mutually exclusive, hence the design of the facility is based on a trade-off activity aiming at an effective compromise. Preliminary dome design has been the result of a spread combined analysis performed at RF, thermal and structural level. The following section provides the most relevant results of the multi-physics design considerations. Also some details about the heating, cooling and moisture removal techniques implemented in the solution are provided.

A. *Material selection*

Foams, honeycombs, composite materials are typically considered in dome technologies. Composite materials offer high mechanical strength with a limited thickness but are mostly characterized by high dielectric constants and significant loss tangent. Foams belong to the family of Polyurethanes and present a wide and versatile industrial application. They represent the best choice for RF application due to their low dielectric constant (ε_r~1) over the frequency. Despite presenting poor mechanical properties, they show appreciable structural characteristics such as isotropy and thermal insulation. Aramid-based honeycombs are also used for RF applications and provide good electrical and mechanical properties, but they suffer from anisotropy (waveguide type behavior at mm-wave), due to the presence of the cells [5].

For the above reasons, Rohacell foam has been chosen for this application, providing high frequency transparency and good thermal insulation. Among the several types of Rohacell, 51-HF model represents a good compromise between electrical and mechanical properties. Datasheet of Rohacell 51-HF manufactured by EVONIK™ [6] reports its typical electric and mechanical properties (Table I. , Table II. , [7]). However, the knowledge of the electrical properties of the material is limited up to 26.5 GHz while the mechanical features are available only at room temperature, not in high temperature conditions. For these reasons, specific testing campaigns are currently in progress to characterize the material electrically, up to 50 GHz, and mechanically, evaluating tensile and compressive strength @ +120°C.

TABLE I. ROHACELL 51-HF ELECTRICAL PROPERTIES (EVONIK™)

Freq [GHz]	Dielectric constant	Loss Tangent
2.5	1.057	< 0.0002
5	1.065	0.0008
10	1.067	0.0041
26.5	1.048	0.0135

TABLE II. ROHACELL 51-HF MECHANICAL PROPERTIES (EVONIK™)

Density	kg/m³ lbs/ft³	52 ± 12 3.25 ± 0.75
Compressive Strength	MPa psi	0.9 130
Tensile Strength	MPa psi	1.9 2.75
Tensile modulus	MPa psi	70 10150
Elongation at break	%	4
Shear Strength	MPa psi	0.8 116
Shear Modulus	MPa psi	19 2755
Thermal Expansion Coefficient	1/K·10E-5	3.34

B. *Thermal analysis*

The main purpose of the thermal analyses is to determine the dome minimum thickness to avoid condensation build-up on its outer surface. In case of icing, the measurement accuracy would be significantly impacted. The thermo-fluid dynamic calculations have indicated that a 100mm thick panel of Rohacell 51-HF provides the necessary insulation (with margin) between the thermal test volume and the rest of the HERTZ chamber, assuming a background temperature of 23°C and 60% humidity (worst case condition). The design is done in such a way that the "dew point" of 14.83°C is taken into account, ensuring that for the two extreme temperature cases, no icing nor condensation occur (Figure 2.).

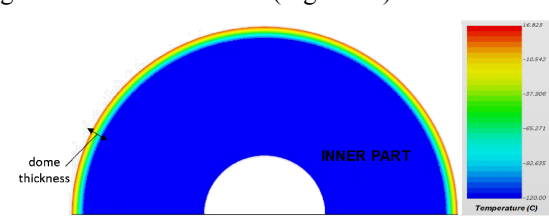

Figure 2. Preliminary thermal analysis: simplified dome structure with -120°C inner termperature.

C. *Dome design*

Some different geometries of the covering structure have been investigated in detail. As a compromise between multi-physics parameters and manufacturing constraints, the most suitable geometry has a faceted structure in Rohacell 51-HF panels, with a base of 2.8m diameter and 2m tall. Panels will be joined together by means of glue layers. A sketch of the dome structure is reported in Figure 3. . The inner volume is equivalent to a half sphere of approx. 2.8m diameter, while the inner dimensions allow to test an AUT with maximum diameter of 2.4m.

In suck a kind of enclosing structure, junctions between panels play a very relevant role because provide stability to the whole framework but, at the same time, represent high dielectric constant regions that can strongly affect the RF performance. A preliminary estimation has led to a definition of 25 junctions, but a more accurate analysis aimed at the evaluation and minimization of their electromagnetic influence will be conducted in a future detailed design stage.

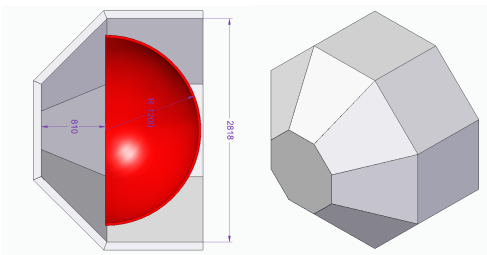

Figure 3. Layout of the faceted dome structure.

D. *Structural analysis*

Concerning the structural analyses, the assessments have been performed considering simplified geometries, with material values declared by the supplier and with preliminary constraint conditions. Analysis have been carried out at ambient temperature. Conversely, since the thermal properties of Rohacell material at +120°C are unknown, conservative estimations have been taken into account for the thermal stress of the material at extreme temperature. It should be noted that the reported results provide a rough indication of the structural behavior, still subject to detailed design.

Analyses shows that the structure exhibits a 3mm maximum displacement located to the top of the dome structure, corresponding on a 0.25% displacement on a 1.25m top panel (Figure 4.). The maximum Stress of Von Mises achieved is equal to 0.0219 MPa, placed on the joint constraints between the vertical support panels and the dome itself. The support panels allow to concentrate the stress on the base and not on the dome structure. The stress of Von Mises on the middle of the dome structure is approximately 0.0088 MPa (70% less than the stress). Overall mass of the dome is 110 kg approximately.

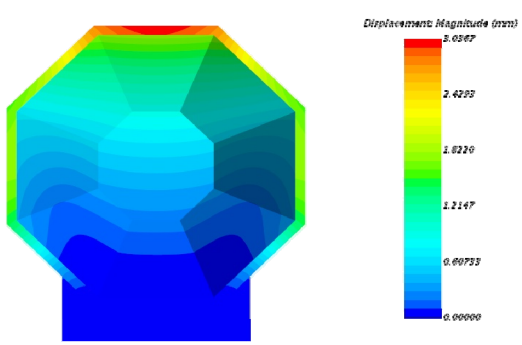

Figure 4. Simulated displacement (back view of the dome with dielectric support structure).

E. *Heating, cooling and moisture removal*

The heating system is based on wire heaters, electrical resistors that converts an electric current into heat (Joule heating). The heat is transmitted by convection and radiation. An appropriately selected air ventilation system allows to provide uniformity of temperature across the AUT within +/- 2 °C. In addition, since the connection between the AUT and the positioner is carried out by flanged stand-off, the use of electrical heaters avoids the thermal impact on Φ-axis motor.

The heating wires increase the surface temperature up to +22°C and avoid the cooling conduction from the internal volume of the dome to the outer part. In such a case no build-up of water and frost will occur. A sketch of this configuration is reported in Figure 5. .

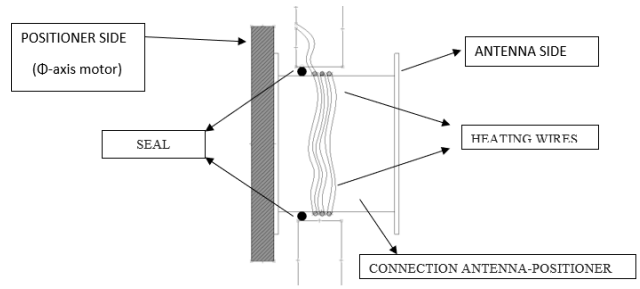

Figure 5. Sketch of the AUT-positioner connection with heating wires.

Cooling is provided by means of a forced ventilation cooling system based on liquid nitrogen. The main advantage of the liquid nitrogen (LN2) cooling system is to have enough cooling power at -120°C, to compensate the thermal dissipation of the dome, AUT and air treatment unit and to have enough margin to reach the minimum temperature of -120°C.

Moisture is avoided injecting gaseous Nitrogen (GN2) inside the air treatment. The continuous flow of GN2 ensures an overpressure inside the dome, both during temperature stabilization and during cooling/heating.

III. ELECTROMAGNETIC ANALYSES

The requirement of covering a large operational bandwidth (0.4 – 50 GHz) within a single test facility makes the design challenging. The facility should also be multi-purpose and allow the testing of a wide variety of AUTs with reasonable measurement accuracy. In the study, an antenna farm consisting of three typical AUT's (Table III.) has been identified and classified on the basis of the directivity levels: an Open Ended Waveguide (7dBi) as Low Gain Antenna (LGA), a Standard Gain Horn (18dBi) as Medium Gain Antenna (MGA) and a Prime Focus Reflector (45dBi) as High Gain Antenna (HGA).

Starting point of the RF analysis has been a preliminary evaluation of the reflectivity of 100 mm thick Rohacell HF 51 panels. This thickness was found in the thermal analysis as the minimum to avoid condensation. The scattering parameters of this layout have been evaluated implementing simplified analytical models based on the transmission matrices for plane-wave incidence.

Further analyses, including the dome shape, have been performed by means of electromagnetic simulation tools with appropriate computational methods: Time Domain method for low and medium gain antennas, and a hybrid approach (based on Method of Moments and Time Domain) for high gain antennas [8].

TABLE III. AUT SIMULATED FOR EACH DOME STRUCTURE.

	Directivity	Freq Band	Method of analysis	AUT	Performance indicator
LGA	7 dBi	L	Time Domain	Open Ended WG	ENL, S11
MGA	18 dBi	X	Time Domain	Standard Gain Horn	ENL, S11
HGA	45 dBi	Ka/V	Method of moments / Time Domain	Prime Focus Reflector	ENL

RF analyses conducted with the Low Gain Antenna (1 – 1.5 GHz) and Medium Gain Antenna (7 – 10 GHz) have shown no major impact of the dome both on return loss, radiation patterns and main radome performance indicators (boresight error, Side-Lobe Level degradation, XPD and Gain reduction). In Figure 6. and Figure 7. , the radiation pattern of the LGA and MGA enclosed in the dome are shown, compared with the reference case (W/O the dome). A further evidence of the extremely low impact of the dome on low and medium gain is given by a comparison between a linearly polarized antenna aligned with the panel junction and the same antenna aligned with the center of a panel. Return loss, directivity radiation patterns evaluated for azimuthal and elevation cuts have demonstrated the dome does not have any impact on the performance of the enclosed antenna. Conversely, for the high gain AUT, the system seems to be more sensitive to the dome. Analyses performed with a Prime Focus Reflector (40 GHz) show that the dome has a noticeable impact, experiencing a reduction in the AUT boresight directivity with respect to the absence of dome (Figure 8.). The reduction has been quantified in 1.1 dB approximately both on co-polar and cross-polar components and on main azimuthal cuts (φ = 0°, 45°, 90°).

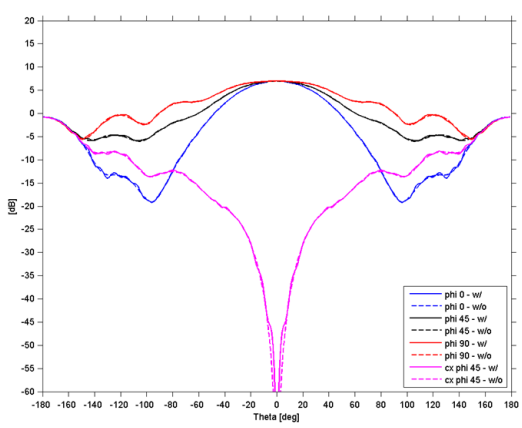

Figure 6. Directivity radiation pattern cuts of the low gain antenna. Comparison W/ and W/O the dome for different azimuth cut at 1.4GHz.

The modeling of the dome has been further refined by including a back panel to enclose the test area and a dielectric support structure, to provide robustness and allow to compensate for the thermal expansion of the dome (Figure 9.). It is interesting to note that the back panel, modeled as a flat thick plate material (ε_r=4) has a relevant impact on the radiative performance of the AUT (Figure 10.). Directivity patterns are significantly rippled and show a directivity drop in correspondence of a field of view of +/- 20° across boresight.

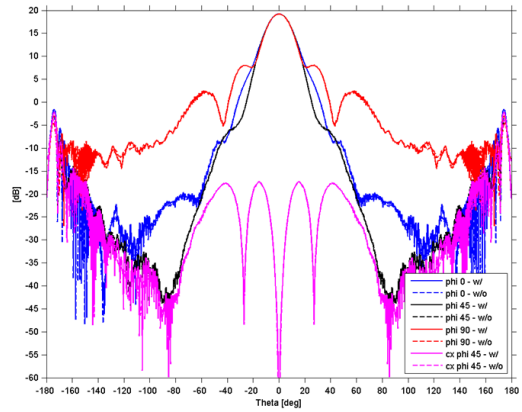

Figure 7. Directivity radiation pattern cuts of the medium gain antenna. Comparison W/ and W/O dome for different azimuth cut at 9 GHz.

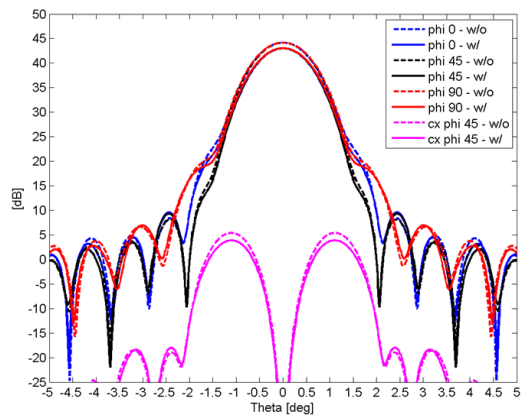

Figure 8. Directivity radiation pattern cuts of the high gain antenna. Comparison W/ and W/O the dome for different azimuth cut at 40GHz.

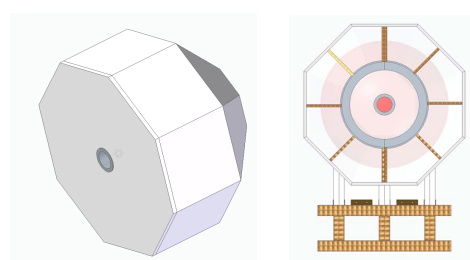

Figure 9. Sketch of the dome with back panel to enclose the test area (left), support structure (right).

This is due to a standing wave effect between the front radiation of the AUT and its back-radiation reflected by the dielectric flat plate. Consequently, besides an optimization of the shape and material, the detailed design of the back panel will consider a treatment with absorbers suitable for use in extreme high/low temperature environment.

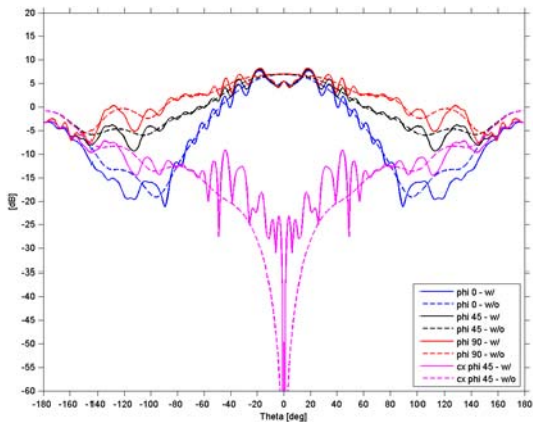

Figure 10. Impact of the back panel on low gain antenna. (W/) Results with dome and back layer. (W/O) Results without dome and back layer.

Finally, the simulated RF performance of the three antennas enclosed by the designed dome have been evaluated in terms of Equivalent Noise Level (ENL) by means of the following formula:

$$ENL = 20 * \log\left[RMSE\left(\frac{Dir_{co,xp} - Dir_{refco,xp}}{Dir_{co,refboresight}}\right)\right]$$

where $Dir_{co,xp}$ is the simulated pattern (W/ dome) and $Dir_{refco,xp}$ is the reference simulated pattern (W/O dome) [9] [10] [11]. The computation takes in account the co-polar component and it is related to the main azimuthal cuts (φ = 0°, 45°, 90°).

TABLE IV. ENL OF AUTS CALCULATED FOR DIFFERENT AZIMUTH CUT

	Low Gain Antenna		**Medium Gain Antenna**		**High Gain Antenna**	
φ (deg)	**Co-Pol (dB)**	**Cx-Pol (dB)**	**Co-Pol (dB)**	**Cx-Pol (dB)**	**Co-Pol (dB)**	**Cx-Pol (dB)**
0	-49.2	<-60	-49.1	<-60	-35.1	<-60
45	-49.2	-51.0	-49.1	-49.1	-35.1	-36.0
90	-46.0	<-60	-47.6	<-60	-35.0	<-60

As shown in Table IV. , the computed ENL is always better than 35 dB (worst case) and 50 dB on average. This value represents an excellent correlation between the two considered situations [9] [10], furtherly demonstrating the suitability of the designed dome at RF level.

IV. CONCLUSIONS

The paper has described the design of a novel test facility to evaluate AUT radiation pattern characteristics in thermal conditions, as an add-on feature to the ESA-ESTEC Hybrid European RF and Antenna Test Zone (HERTZ). The described system consists of a RF transparent, thermally insulated dome surrounding the AUT, connected to the thermal unit, that allows heating (+120°C) and cooling down (-120°C) the antenna under test, working in the 0.4 – 50 GHz bandwidth. The system allows the free rotation of the Phi and Theta Axis, while cooling or warming the AUT during a SNF acquisition.

A concept design has been proposed to represent the system in development. The framework is composed as follows a faceted dome in Rohacell 51-HF, a dielectric support structure and a rear panel connected to the positioner. Extreme temperature conditions are achieved by means of wire heating (hot) and LN2 (cold). In addition, an air treatment unit based on GN2 allows to remove moisture.

The dome has been preliminarily designed after a jointly analysis at RF, thermal and structural level. The proposed model will be furtherly improved in a detailed design phase, once dome material will be appropriately characterized at electrical and mechanical level.

ACKNOWLEDGEMENT

This activity has been funded and developed in the frame of ESA Contract N. 4000123995/18/NL/AF, “HIGH ACCURACY COHERENT ANTENNA TESTING OVER TEMPERATURE”.

REFERENCES

[1] O. Breinbjerg, “Spherical Near-Field Antenna Measurements - The Most Accurate Antenna Measurement Technique”, IEEE International Symposium on Antennas and Propagation (APSURSI), 2016, Puerto Rico;

[2] IEEERecommended Practice for Near Field Antenna Measurement, IEEE Std. 1720-2012;

[3] IEEE Standard Test Procedures for Antennas, IEEE Std. 149-1979;

[4] J. E. Hansen (ed.), Spherical Near-Field Antenna Measurements, Peter Peregrinus Ltd., on behalf of IEEE, London, United Kingdom, 1988

[5] J. Kozakoff, Analysis of Dome-enclosed antennas, Second edition, Artech House, Norwood, U.S.A., 2010;

[6] Evonik, official Web site: https://corporate.evonik.com/en/ ;

[7] Rohacell HF, official Web site: https://www.rohacell.com/product/rohacell/en/products-services/rohacell-hf;

[8] CST Studio Suite ™, https://www.3ds.com/products-services/simulia/products/cst-studio-suite;

[9] M. A. Saporetti et al., "Measurements and simulations correlation of high reliability reflector antenna," 2016 10th European Conference on Antennas and Propagation (EuCAP), Davos, 2016, pp. 1-5;

[10] M. Alberica Saporetti, L. Foged, M. Sierra Castaner, S. Pivnenko, R. Cornelius and D. Heberling, "Description and Results: Antenna Measurement Facility Comparisons," in IEEE Antennas and Propagation Magazine, vol. 59, no. 3, pp. 108-116, June 2017;

[11] M. A. Saporetti et al., "International facility comparison campaign at L/C band frequencies," 2017 Antenna Measurement Techniques Association Symposium (AMTA), Atlanta, GA, 2017, pp. 1-6.